MAPPING AND ASSESSMENT OF DAMAGES OF TYPHOON OMPONG IN ILOCOS REGION USING VIIRS NIGHTTIME LIGHTS AND SENTINEL-1 SAR IMAGERY

R. L. Castillo [1, a], C. M. Fiel Jr. [1, b], R. Matiga [1, c], J.F. Paganao [1, d], J. Teologo [1, e]

[1]Department of Earth and Space Science, Rizal Technological University, Mandaluyong City, Philippines

[a]2022-201649@rtu.edu.ph [b]2022-201622@rtu.edu.ph [c]2022-205382@rtu.edu.ph [d]2022-203311@rtu.edu.ph [e]2022-205382@rtu.edu.ph

KEY WORDS: Disaster Mapping**,** Disaster Assessment, Nighttime light, SAR, VIIRS, Typhoon OMPONG, Sentinel-1 Algorithm

ABSTRACT:

The aftermath of Typhoon Ompong's recent impact on a substantial portion of the northern regions in the Philippines has been marked by widespread disruptions, leading to significant economic challenges. This study addresses the multifaceted repercussions, primarily focusing on the damages inflicted on infrastructures, establishments, and families. Employing a comprehensive approach, geospatial information is harnessed through Rapid Damage Assessment techniques to provide a nuanced understanding of the extent of the devastation. Central to this effort is the utilization of Sentinel-1 synthetic aperture radar (SAR) imagery. This choice is grounded in the open-access availability of the data, its high temporal resolution facilitating pre- and post-disaster image comparisons, and its relative independence from atmospheric conditions, ensuring data integrity even in the presence of cloud cover. The methodology involves a meticulous analysis of complex coherence correlation derived from stacks of pre- and post-disaster SAR images for effective change detection. This comprehensive approach allows for both qualitative and quantitative evaluations to validate the results. Noteworthy observations emerge from the examination of pre-typhoon and post-typhoon preprocessed SAR images, conducted using 'IW' (Interferometric Wide Swath) instruments. Analysis of pixel mean values in various transmitter-receiver polarization modes—'VV' (vertical-vertical) and 'VH' (vertical-horizontal)—reveals fluctuations in SAR image creation. The study underscores the impact of transmission modes and the timeline of image acquisition on the observed values. The resulting maps from this research are anticipated to play a pivotal role in the ongoing efforts to rehabilitate the areas affected by Typhoon Ompong. The study proposes future work that includes additional ground validation efforts and the exploration of alternative datasets and methodologies to further enhance the precision and applicability of rapid damage assessment maps.

1. BACKGROUND

1.1 Introduction

On September 12, 2018, Typhoon Mangkhut or locally known as Ompong entered the PAR and made a landfall in the province of Cagayan late September 14, 2018, as a Category 5 super typhoon with a maximum sustained winds of 205 kilometers per hour (kph) near the center and gustiness of up to 285 kph. Typhoon Ompong traveled in a west-northwestward trajectory primarily affecting Central Luzon. According to the National Disaster Risk Reduction and Management Council (NDRRMC 2018), approximately 510,151 families or 2,148,059 individuals across Regions NCR, I, II, III, CALABARZON, MIMAROPA, and CAR were affected by the typhoon, with estimated direct damages of 33.6 billion pesos or US$623 million to infrastructure and agriculture. With PHP1.65 billion in damage to agriculture and PHP52 million to infrastructures as per the Provincial Disaster Risk Reduction and Management Office (PDRRMO 2018), the Ilocos region is one of the provinces that suffered major damages from the typhoon.

Part of the country's disaster response management is the creation of damage assessment maps. These maps are used to record the scope of the damage, assess what areas need the most aid, and assist the government's effort in facilitating effective and efficient response and rehabilitation of the areas. According to Announcement Philippines 2022, typhoon Ompong ranks 5th in the most destructive typhoon that made landfall in the Philippines based on its destructiveness, and economic damages. Given the damages of typhoon Ompong, the recorded information about the typhoon is still insufficient making it unviable to be a reference for the future typhoon response.

Satellites can gather different types of data from broad areas and store them on Earth data storage. Due to these, satellites particularly used for remote sensing are highly used for damage mapping, and assessment, for various disasters. For instance, various technologies such as optical imaging, synthetic aperture radar (SAR), and light detection and ranging (LiDAR) have been employed to create maps of the damages because of earthquakes, landslides, explosions, tsunamis, typhoons, and floods (Van Westen, 2020; Agapiou, 2020). Synthetic aperture radar (SAR) capabilities of detecting infrastructure, amount of moisture, water level, effects of natural or human activities, and changes in the Earth's surface after events such as earthquakes, make it a popular and effective tool for remote sensing. SAR ability to yield high-resolution, day-and-night, and weather-independent images caters to variety of application including geoscience, climate change research, environmental monitoring, Earth system observation, 2-D and 3-D mapping, change detection, 4-D mapping, and even extends to planetary exploration (Moreira et al. 2020). On the other hand, visible Infrared Imaging Radiometer Suite (VIIRS) instrument ability to collect visible and infrared images, provides data for measuring cloud and aerosol properties, ocean and land surface temperature, and nighttime lights, etc. Nighttime lights indicate the result of satellite observation of the artificial lighting of human activities on the Earth from space during the night, which provides the excellent opportunity to determine their position, pattern, density, and spatial distribution (Panic et al. 2022). The VIIRS system can collect unprocessed data, which can then be employed to generate precise global radiance maps of human settlements illuminated by electric lights, both on a monthly and yearly scale, with a scientific rigor (Elvidge et al. 2017). This concludes the advantages of utilizing SAR and VIIRS datasets to produce a damage assessment map for typhoons in dense areas such as cities, in which optical images from satellites are blocked.

The researchers utilized datasets from Sentinel-1, and NOAA-20 to identify, assess, and map damages caused by typhoon Ompong on major cities of Ilocos region. Sentinel 1 SAR and NOAA-20 VIIRS datasets are gathered and processed through the Google Earth Engine. Images gathered and processed from SAR will be used to map the damage in infrastructure by comparing the pre and post typhoon images. On the other hand, VIIRS images will be used to map as well as quantify the amount of nighttime light intensity pre and post typhoon. Lastly, the research will also compare the quantitative data from SAR and VIIRS in order to create a critical and accurate analysis of the damages from the typhoon.

1.2 Study Area

The study areas identified for this research are the capital cities of provinces in Ilocos where Typhoon Ompong passed during its course within the Philippine area of responsibility (PAR), namely, the Provinces of Ilocos Norte, Ilocos Sur, La Union, and Pangasinan (Fig. 1).

These study areas were chosen due to the following factors: (a) nighttime light intensity and density of infrastructure pre-typhoon, (b) availability of Sentinel-1 and NOAA-20 data that is near the time before after the typhoon past through, (c) scope of estimated damages by the NDRRMC, and (d) ability of artificial satellites to detect damages brought by natural disasters.

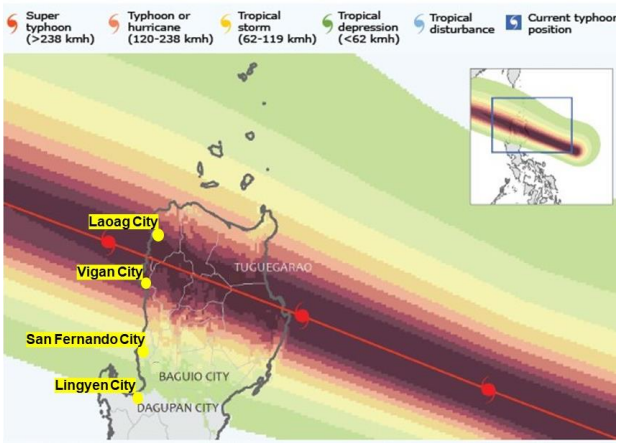

Figure 1. Path of Typhoon Ompong which affected areas in the Central Luzon Philippines. Points indicate the location map of the study areas (i.e., selected cities in Ilocos Norte, Ilocos Sur, La Union, and Pangasinan). Adapted from (OCHA, 2018).

1.3 Data Sources

Sentinel-1 SAR and NOAA-20 VIIRS data used in this study, such as the images, and graphs were gathered processed and from the Google Earth Engine website (https://code.earthengine.google.com/). Final processing of images processed in the Google Earth Engine was done in the QGIS software (https://qgis.org/en/site/). Lastly, datas from typhoon Ompong such as Typhoon trajectory map, and strength of typhoon was collected from the United Nations Office for the Coordination of Humanitarian Affairs (https://www.unocha.org/).

2. METHODOLOGY

2.1 Related works

Damage assessment and mapping post disaster is a standard procedure done by various sectors such as the government and academe, to provide a detailed analysis of the impact of the disaster. As such downstream data gathered through remote sensing from satellites has been long utilized to create damage assessments maps. SAR and VIIRS instruments of certain satellites are highly used in these processes because of their capability of providing accurate Earth data unobstructed.

a. Satellite Aperture Radar

Synthetic aperture radar pertaining to a manner for manufacturing quality-solution images from an intent-limited radar structure (NASA). It is an active sensor that first transfers microwave signals and then collects back the signs that are returned or dispersed from the Earth's exterior (Alaska Satellite Facility). SAR imageries are mainly not affected by the atmospheric and environmental characteristics, for example, cloud cover, rain, sun illumination, etc., which provides this data type acceptable for emergency rapid response mapping in times of disasters and tragic events where secular availability is of greatest importance (Ge, et. al., 2020; Brunner et. al., 2010). To assess and respond to climate change, ecosystem loss, natural disasters, agriculture, flood, land subsidence, wildfire and many more, SAR has a wide range of applications that provides additional information (Cepeda R 2020). By gathering pre-typhoon and post-typhoon images, co-registering them to a master image, and controlling the coherence of the stacked image, for instance, Sentinel-1 SAR images were used to map potentially destroyed areas in the severely affected Caraga Region before and after typhoon images (Bolanio et al., 2022).

b. Visible Infrared Imaging Radiometer Suite

According to the National Environmental Satellite, Data, and Information Service the Visible Infrared Imaging Radiometer Suite (VIIRS) instrument gathers global observations of the land, atmosphere, cryosphere, and oceans and simultaneously collects visible and infrared images. The VIIRS sensor technology monitors and gathers worldwide satellite observations covering land, ocean, and atmosphere in visible and infrared wavelengths (NASA). Higher dynamic range, on-board calibration, and several optical bands that are essential for recognizing among different light sources are accessible by VIIRS (Linden et al. 2018). Furthermore, typhoon-related interruptions in power and the aftermath of typhoons and other catastrophic events have been assessed using daily Nighttime light (NTL) data from both NPP-VIIRS DNB and DMSP-OLS (He et al 2019).

2.2 SAR Data Processing

Fig. 2 shows the SAR data processing methodology applied in this study. Primarily the SAR data processing was programmed in the Google Earth Engine (GEE) terminal using the JavaScript language.

First, the targeted Sentinel 1 SAR datasets were retrieved from the ESA Copernicus, using the GEE. Two datasets of images were retrieved in the GEE, the pre disaster which are the images a week before the typhoon to the day of disaster (Sept. 8 – 14), and the post disaster which are the images from a day after to a week following the typhoon (Sept 16 – 21). The available images in the targeted timeframe were automatically stacked in GEE. Second, the datasets from GEE underwent the process of Metadata Filtering to determine the sensor and filter for the image, it includes different properties namely Transmitter, Receiver, Polarization Instrument, Mode Orbit, and Properties Pass, these properties calculate observations composites displayed on the map. The Google Earth Engine uses an imagery dataset that consists of Level-1 Ground Range Detected (GRD) processed to deflect coefficient (σ°) in decibels (dB). GEE uses the preprocessing steps same as the process used in Sentinel-1 Toolbox when using Sentinel Application Platform (SNAP).

To enhance the images as such to increase its quality, accuracy, and usability, making them applicable to use for damage assessment mapping, the images are preprocessed. In which the images are programmed and underwent the processes of:

1. Application of Orbit File- Applying orbit files involves using precise satellite orbit information to correct geometric distortions caused by the satellite's movement.
2. GRD Border Noise Removal- eliminate artifacts or inconsistencies at the edges of the image, enhancing the overall image quality.
3. Thermal Noise Removal- used to reduce or eliminate this noise, enhancing the clarity of the SAR image.
4. Application Of Radiometric Calibration Values- Calibration values are used to convert raw signal values into calibrated values.
5. Terrain Correction (Orthorectification) - involves the removal of these distortions, making the image geographically accurate.

Since the dataset used does not bound the filter on the shapefile imported, the researchers used the line drawing in GEE to isolate and emphasize the study areas.

After the images are preprocessed each set of pre disaster and post disaster images of each city are then downloaded and quantified. The pixels from each image are categorized and counted to quantify the data and proceed to create a pixel mean chart. The data from the pre-typhoon and post-typhoon timelines were compared and analyzed by the researchers. Lastly, discussion of interpretation of the data once an accurate depiction of the data that had been achieved.

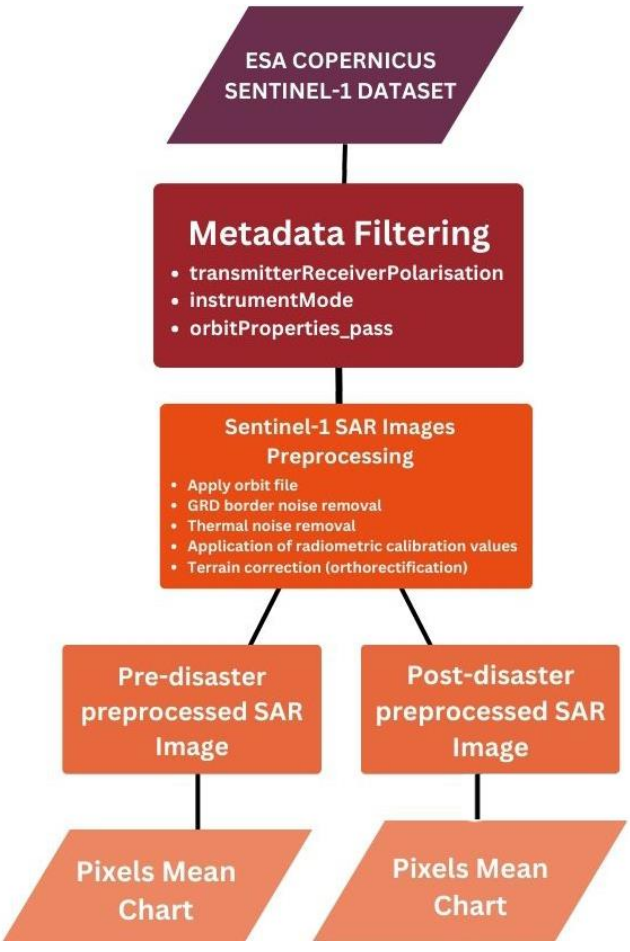

Figure 2. An overview of the SAR data processing framework in which Sentinel 1 images are processed to acquire dataset and images for damage assessment maps, and analysis.

2.3 VIIRS Data Processing

Fig. 3 shows the VIIRS data processing methodology applied in this study.

First, the researchers retrieve shapefile datasets from the Humanitarian Data Exchange. Next, the various datasets under the Philippine - Subnational Administrative Boundaries were imported into Quantum Geographic Information System (QGIS), the targeted cities were chosen and exported into a single shapefile one by one. Shapefiles of cities were then imported into Google Earth Engine Assets. After that, the datasets were programmed to generate an image in the Google Earth Engine, with VIIRS band represented by distinct colors representing different values. Following that, the time series analysis focuses on a span of seven days before and seven days similar timeframe in the SAR datasets, after Typhoon Ompong for the specified cities in Region I. The results of Day-Night Band (DNB) and sensor radiance at 500m time-series for different cities are aggregated. A line chart is then created from the quantified data to visualize and analyze the NTL data before and after the typhoon hit in the capital cities of Region I. Lastly, following data collection, comparison, and interpretation, conclusions were drawn from the analysis of charts and radiance values.

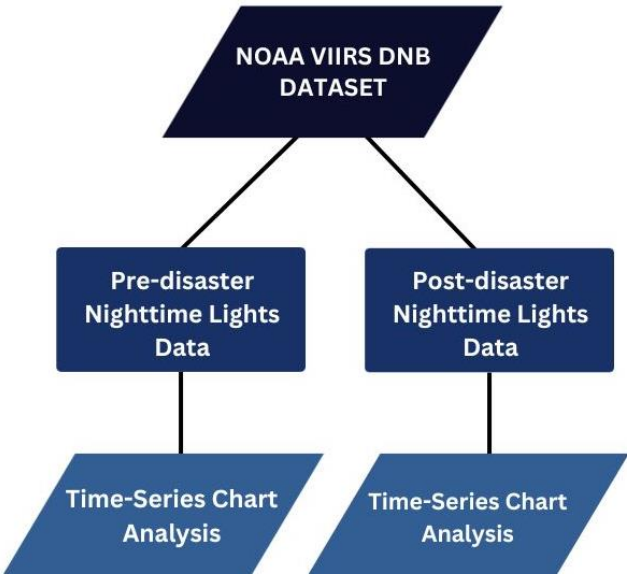

Figure 3. An overview of the VIIRS data processing framework in which NOAA images are retrieved and shaped to acquire nighttime light images and dataset.

3. RESULTS AND DISCUSSION

3.1 SAR Damage Assessment Maps

Figures 4-7 show the output SAR images after the preprocessing, displaying the pre and post typhoon images of the specified areas. Tables 1-4 display the quantified SAR pixel data used for graphing. The researchers noticed that there are differences between the pre-typhoon and post-typhoon preprocessed SAR images. The instruments used are 'IW' (Interferometric Wide Swath). The data collected in this study's pixels mean of images in various transmitter Receiver Polarization modes—'VV', 'VH'—showed that both modes—VV (vertical-vertical), which transmits and receives vertical waves, and VH (vertical-horizontal), which transmits and receives horizontal waves—create SAR images (Capella Space, 2022). Depending on the mode and timeline when the photos were taken, values can be seen to rise or fall.

In Laoag City, the post-disaster image's vvIwAscDescMean value decreased by decimals. The pre-disaster image has a higher value by decimal in vhIwAscDescMean. Regarding vhIwAscMean, there is no distinction between the pre- and post-disaster images. Prior to the disaster, the pixel mean image of the vhIwDescMean value was higher.

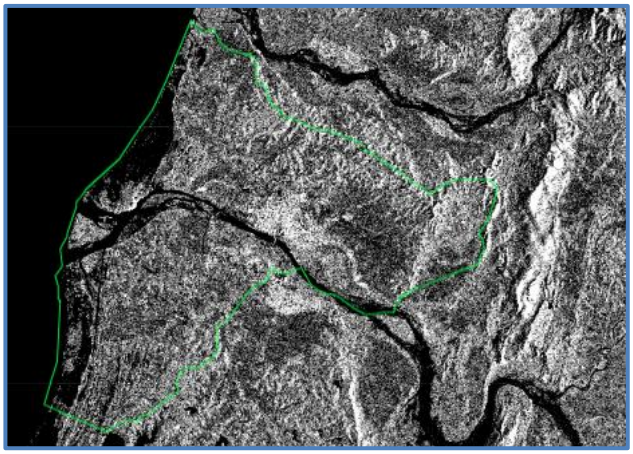

Figure 4. Pre-typhoon preprocessed image of Laoag city (enclosed by green line drawing) generated by Google Earth Engine with a Sentinel-1 Algorithm 'COPERNICUS/S1_GRD'.

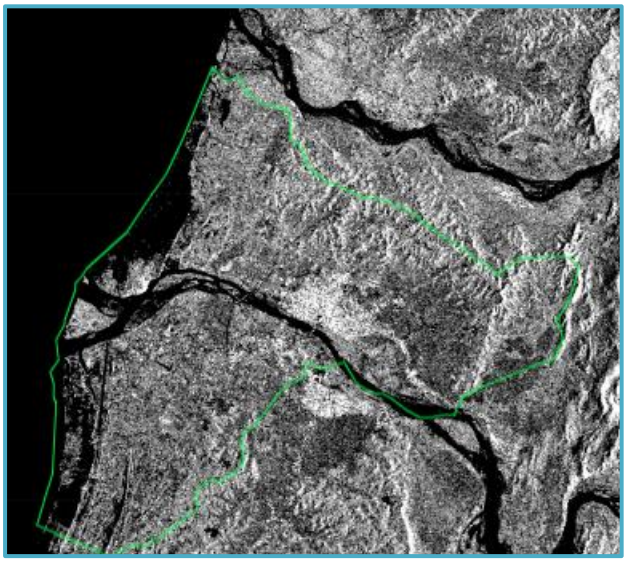

Figure 5. Post-typhoon preprocessed image of Laoag city (enclosed by green line drawing) generated by Google Earth Engine with a Sentinel-1 Algorithm 'COPERNICUS/S1_GRD'.

Laoag City: Pre-disaster	**Pixels**
vvIwAscDescMean	VV: -11.323625722956074
vhIwAscDescMean	VH: -19.243896778596696
vhIwAscMean:	VH: -17.541154749127816
vhIwDescMean	VH: -19.243896778596696
Laoag City: Post-disaster	**Pixels**
vvIwAscDescMean	VV: -11.663624237815425
vhIwAscDescMean	VH: -19.294367302788654
vhIwAscMean:	VH: -17.541154749127816
vhIwDescMean	VH: -20.170973579619073

Table 1. Pixels mean values of the preprocessed SAR images on the timeframe. The value is dependent on the Sensor Mode, IW, and the Dual Polarization (VV+VH) in the SAR System.

In Vigan City, the pre-disaster vvIwAscDescMean image value is higher than the post-disaster image. The values of vhIwAscDescMean and vhIwAscMean in the post-disaster image are both greater than those in the pre-disaster image. Additionally, the post-disaster image has a higher decimal value of vhIwDescMean than the pre-disaster image. In comparison to the pre-disaster image, most of the mean values were higher in the post-disaster one.

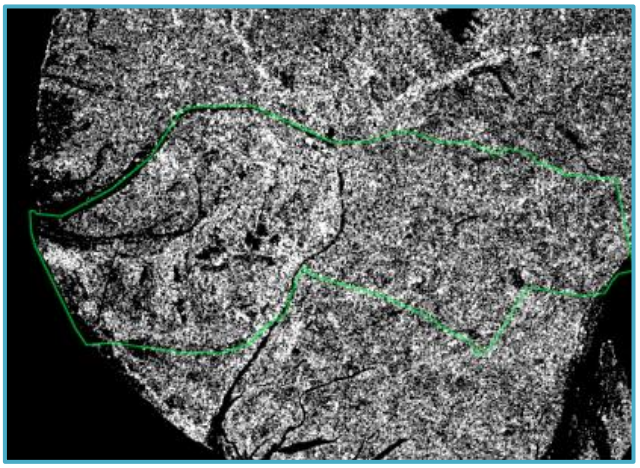

Figure 6. Pre-typhoon preprocessed image of Vigan city (enclosed by green line drawing) generated by Google Earth Engine with a Sentinel-1 Algorithm 'COPERNICUS/S1_GRD'.

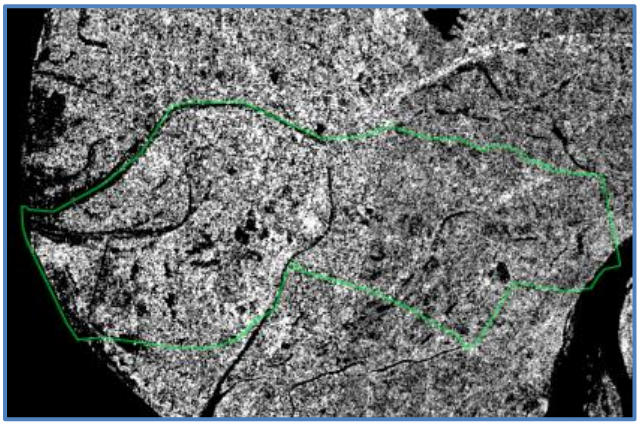

Figure 7. Post-typhoon preprocessed image of Vigan city (enclosed by green line drawing) generated by Google Earth Engine with a Sentinel-1 Algorithm 'COPERNICUS/S1_GRD'.

Laoag City: Pre-disaster	**Pixels**
vvIwAscDescMean	VV: -3.525967940593949
vhIwAscDescMean	VH: -15.340690143300135
vhIwAscMean:	VH: -14.300690143300189
vhIwDescMean	VH: -15.340690143300135
Laoag City: **Post-disaster**	**Pixels**
vvIwAscDescMean	VV: -5.316082196762463
vhIwAscDescMean	VH: -12.920939994422204
vhIwAscMean	VH: -10.736988932703193
vhIwDescMean	VH: -15.104891056141215

Table 2. Pixels mean values of the preprocessed of the SAR images of Vigan City on the specified timeframe. The value is dependent on the Sensor Mode which is the IW, and the Dual Polarization (VV+VH) in the SAR System.

Meanwhile, in San Fernando City, the vvIwAscDescMean value is higher by decimals in pre-disaster image. Contrasting to the post-disaster image, the pre-disaster image's vhIwAscDescMean and vhIwAscMean are higher by 1 negative value. The pre-disaster image's vhIwDescMean, however, has a higher decimal value.

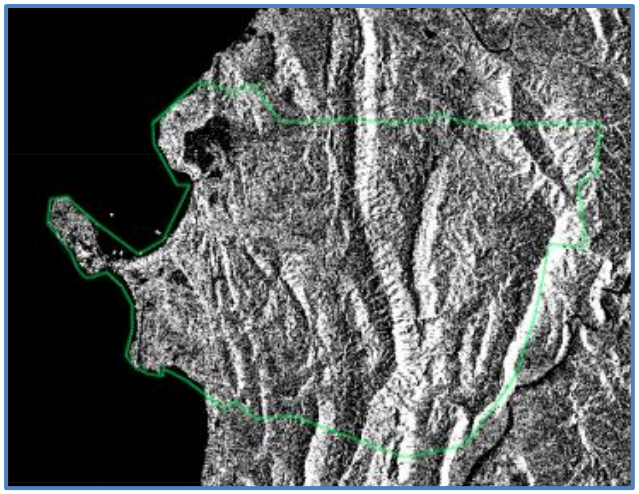

Figure 8. Pre-typhoon preprocessed image of San Fernando city (enclosed by green line drawing) generated by Google Earth Engine with a Sentinel-1 Algorithm 'COPERNICUS/S1_GRD'.

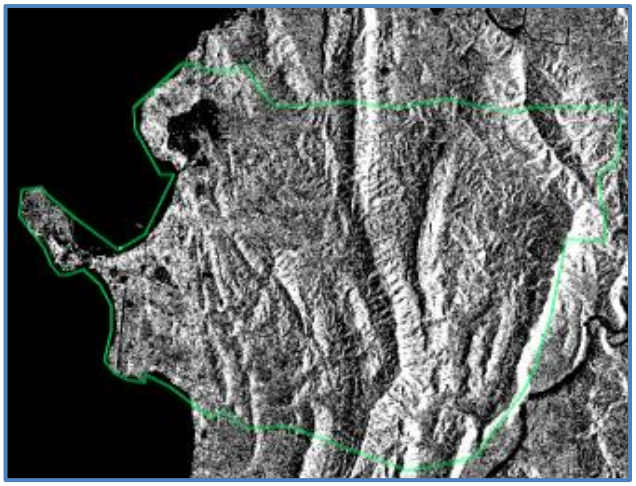

Figure 9. Post-typhoon preprocessed image of San Fernando city (enclosed by green line drawing) generated by Google Earth Engine with a Sentinel-1 Algorithm 'COPERNICUS/S1_GRD'.

San Fernando city: Pre-disaster	**Pixels**
vvIwAscDescMean	VV: -4.051662217781244
vhIwAscDescMean	VH: -12.400780923679955
vhIwAscMean:	VH: -12.456326632645533
vhIwDescMean	VH: -12.456326632645533
San Fernando city: Post-disaster	**Pixels**
vvIwAscDescMean	VV: -4.1033504213437295
vhIwAscDescMean	VH: -13.04467300937106
vhIwAscMean:	VH: -13.163740344330567
vhIwDescMean	VH: -12.985139341891308

Table 3. Pixels mean values of the preprocessed SAR images of San Fernando City on the specified timeframe. The value is dependent on the Sensor Mode, which is the IW, and the Dual Polarization (VV+VH) in the SAR System.

Lastly, the pre-disaster image of Lingayen City has higher values for vvIwAscDescMean, vhIwAscDescMean, and vhIwAscMean. The vhIwDescMean is higher by 1 negative value in the post-disaster image.

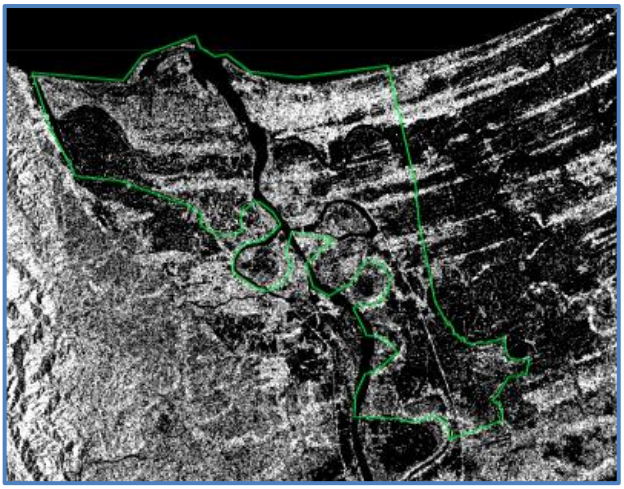

Figure 10. Pre-typhoon preprocessed image of Lingayen city (enclosed by green line drawing) generated by Google Earth Engine with a Sentinel-1 Algorithm 'COPERNICUS/S1_GRD'.

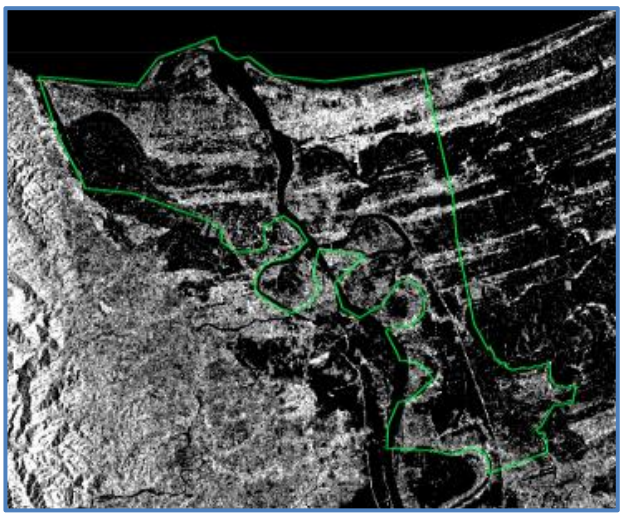

Figure 11. Post-typhoon preprocessed image of Lingayen city (enclosed by green line drawing) generated by Google Earth Engine with a Sentinel-1 Algorithm 'COPERNICUS/S1_GRD'.

Lingayen City: Pre-disaster	**Pixels**
vvIwAscDescMean	VV: -10.203584041375699
vhIwAscDescMean	VH: -16.228291088372977
vhIwAscMean:	VH: -16.107893290938476
vhIwDescMean	VH: -16.228291088372977
Lingayen City: Post-disaster	**Pixels**
vvIwAscDescMean	VV: -8.92867007171725
vhIwAscDescMean	VH: -16.009340948149628
vhIwAscMean:	VH: -16.20432740727624
vhIwDescMean	VH: -15.911847718586323

Table 4. Pixels mean values of the preprocessed SAR images of Lingayen City on the specified timeframe. The value is dependent on the Sensor Mode, which is the IW, and the Dual Polarization (VV+VH) in the SAR System.

Figure 12-13 Shows the summary of the pre and post disaster pixel mean analyze through line graph.

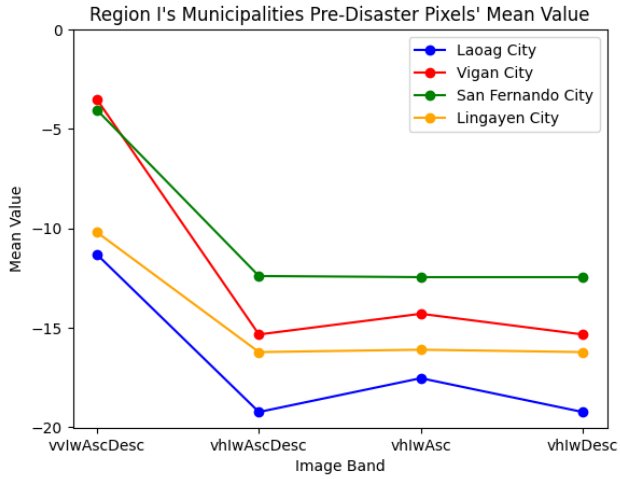

Fig 12. The Pixels mean daily record in selected cities during the post-typhoon (date) provided by the Sentinel-1 Algorithm and is generated by GEE's Inspector at coordinates.

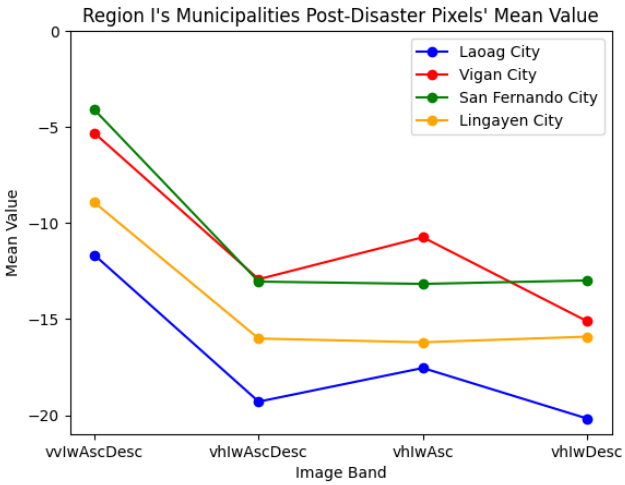

Fig 13. The Pixels mean daily record in selected cities during the pre-typhoon (date) provided by the Sentinel-1 Algorithm and is generated by GEE's Inspector at coordinates.

3.2 VIIRS Nighttime Light Analysis

The time-chart series analysis produced by Google Earth Engine shows that the researchers collected the NTL data seven days prior to and seven days following Typhoon Ompong's landfall. On various days, distinct values of the DNB image bands from the VIIRS moderate-resolution band were observed. The quantified values' ascent and descent over time are depicted in the charts and tables below.

In conclusion, on September 11, 2018, the fourth day before Typhoon Ompong made landfall, the city of San Fernando achieved the highest extracted value of band in its image. The day before the typhoon made landfall, all of the cities' images showed a low band value, indicating the typhoon's upcoming effects. On September 16, 2018, as the typhoon passed through the PAR, all cities were seen to display a descending to ascending value in the image band. On the final day of timeline observation, Laoag City achieved the highest value of the image band, according to the data collected.

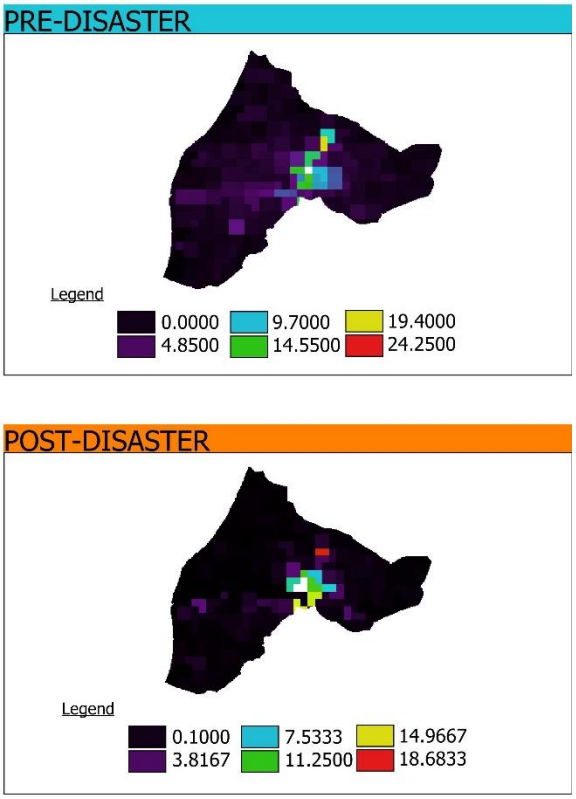

Fig 14. Map Layout made in QGIS of the pre and post-typhoon Nightlight image data in Laoag city generated by Google Earth Engine with VNP46A1: VIIRS Daily Gridded Day Night Band 500m Linear Lat Lon Grid Night dataset.

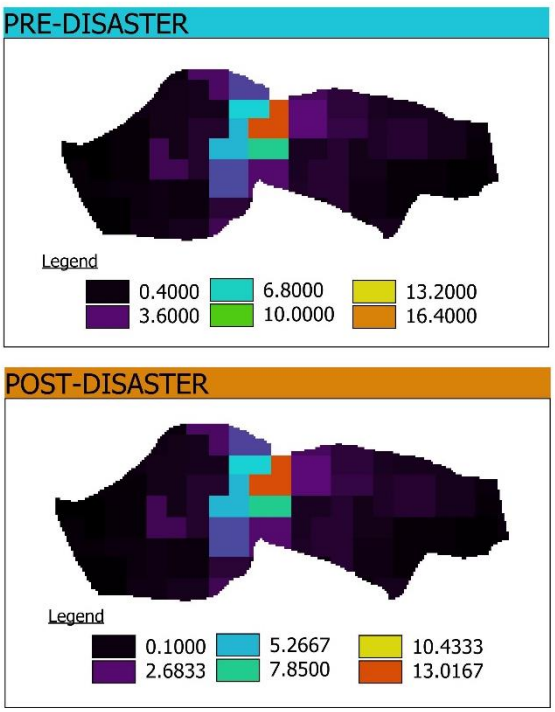

Fig 14. Map Layout made in QGIS of the pre- and post-typhoon Nightlight image data in Vigan city generated by Google Earth Engine with VNP46A1: VIIRS Daily Gridded Day Night Band 500m Linear Lat Lon Grid Night dataset.

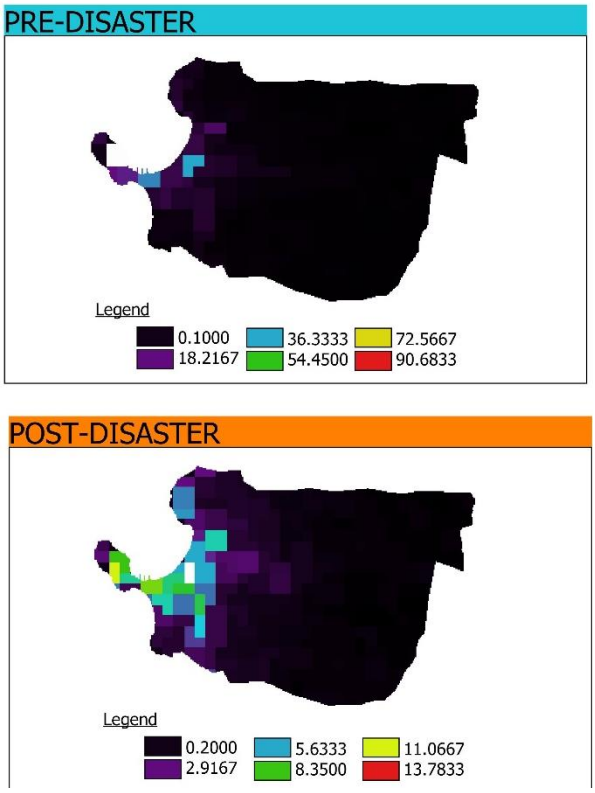

Fig 14. Map Layout made in QGIS of the pre- and post-typhoon Nightlight image data in San Fernando City generated by Google Earth Engine with VNP46A1: VIIRS Daily Gridded Day Night Band 500m Linear Lat Lon Grid Night dataset.

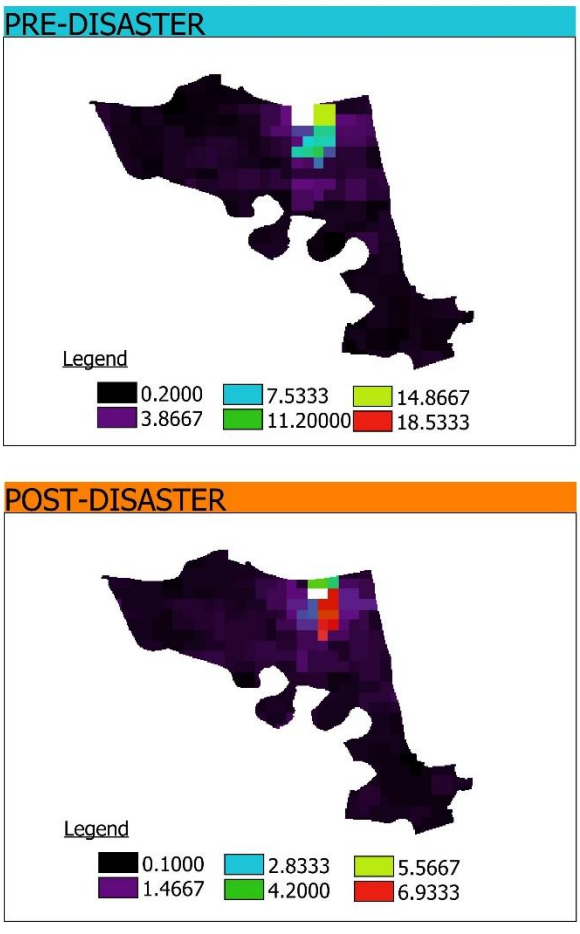

Fig 15. Map Layout made in QGIS of the pre- and post-typhoon Nightlight image data in Lingayen City generated by Google Earth Engine with VNP46A1: VIIRS Daily Gridded Day Night Band 500m Linear Lat Lon Grid Night dataset.

Loc: Laoag City Date: September 08-14, 2018	Corrected NTL Percentage (Pre-disaster)
08	0.498 %
09	1.233 %
10	0.482 %
11	1.972 %
12	1.253 %
13	1.523 %
14	0.459 %

Table 5. The quantified values in % of VIIRS NTL data gathered during the pre-typhoon in Laoag City.

Loc: Laoag City Date: September 16-22, 2018	Corrected NTL Percentage (Post-disaster)
16	0.585 %
17	1.254 %
18	1.037 %
19	1.209 %
20	1.817 %
21	2.953 %
22	4.375 %

Table 6. The quantified values in % of VIIRS NTL data gathered during the post-typhoon in Laoag City.

Loc: Vigan City Date: September 08-14, 2018	Corrected NTL Percentage (Pre-disaster)
08	0.883 %
09	0.948 %
10	0.498 %
11	1.849 %
12	1.423 %
13	0.889 %
14	0.41 %

Table 7. The quantified values in % of VIIRS NTL data gathered during the pre-typhoon in Vigan City.

Loc: Vigan City Date: September 16-22, 2018	Corrected NTL Percentage (Post-disaster)
16	0.634 %
17	1.226 %
18	1.142 %
19	0.947 %
20	1.473 %
21	2.666 %
22	3.907 %

Table 8. The quantified values in % of VIIRS NTL data gathered during the post-typhoon in Vigan City.

Loc: San Fernando City Date: September 08-14, 2018	Corrected NTL Percentage (Pre-disaster)
08	1.373 %
09	1.211 %
10	1.34 %
11	2.25 %
12	1.672 %
13	1.305 %
14	0.53 %

Table 9. The quantified values in % of VIIRS NTL data gathered during the pre-typhoon in San Fernando City.

Loc: San Fernando City Date: September 16-22, 2018	Corrected NTL Percentage (Post-disaster)
16	0.499 %
17	1.726 %
18	1.682 %
19	1.253 %
20	1.695 %
21	2.884 %
22	4.092 %

Table 10. The quantified values in % of VIIRS NTL data gathered during the post-typhoon in San Fernando City.

Loc: Lingayen City Date: September 08-14, 2018	Corrected NTL Percentage (Pre-disaster)
08	0.812 %
09	0.828 %
10	1.028 %
11	1.773 %
12	0.789 %
13	0.695 %
14	0.423 %

Table 11. The quantified values in % of VIIRS NTL data gathered during the pre-typhoon in Lingayen City.\

Loc: Lingayen City Date: September 16-22, 2018	Corrected NTL Percentage (Post-disaster)
16	0.77 %
17	1.395 %
18	1.132 %
19	0.844 %
20	2.317 %
21	2.481 %
22	3.548 %

Table 12. The quantified values in % of VIIRS NTL data gathered during the post-typhoon in Lingayen City.

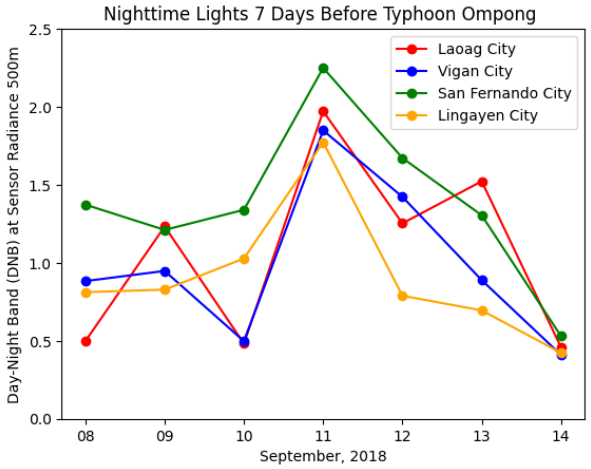

Fig 16. Pre-typhoon daily record of corrected NTL in % based on Day-Night Band (DNB) at Sensor Radiance 500m

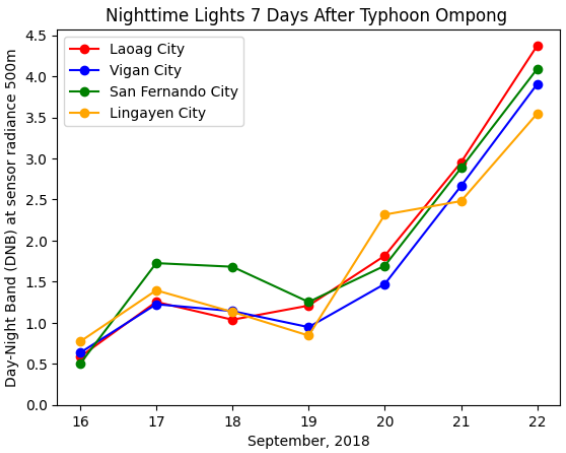

Fig 17. Post-typhoon daily record of corrected NTL in % based on Day-Night Band (DNB) at Sensor Radiance 500m

3.3 Conclusions and Recommendations

The researchers were able to ascertain the recovery pattern timeline for the selected areas by evaluating pre- and post-typhoon effects in multiple areas. The results of this study have been supported by a variety of reliable scientific data sets obtained from various satellites. Tables, charts, and map layouts are provided to reinforce the conclusion.

The preprocessed SAR images and the VIIRS NTL data analysis show a correlation between them in terms of how the results obtained following the typhoon affect each other. The areas affected by the typhoon were demonstrated by the consistency of the data in the ascent and descent graphics. The data collected also shows that there is evidence of the recovery pattern.

It is highly recommended that future researchers who want to expand on and refine this study to preprocess SAR images of a specific area using European Space Agency applications like SNAP or The Sentinel Application Platform. A more accurate data analysis can be obtained by comparing images taken one day prior and the day following the disaster. One of the key components supporting the data correlation is the application of qualitative assessment of damages caused by a disaster. An open source tool called UNOSAT offers photos of specific regions so that one can see the physical consequences of a disaster. To observe the distinct capabilities of the two methods (VIIRS and SAR), additional sets of parameters should be taken into consideration as well.

REFERENCES:

Draper, D. W. (2018, June). Radio Frequency Environment for Earth-Observing Passive Microwave Imagers. *IEEE Journal of Selected Topics in Applied Earth Observations and Remote Sensing*, *11*(6), 1913–1922. https://doi.org/10.1109/jstars.2018.2801019

PAGASA. (2018). *Typhoon Ompong (Mangkhut / 1822) Summary Report*. Weather Division, PAGASA. https://pubfiles.pagasa.dost.gov.ph/tamss/weather/tc_summary/TY_Ompong_MANGKHUT_2018.pdf

DOST-PAGASA. (2018). *DOST-PAGASA ANNUAL REPORT ON PHILIPPINE TROPICAL CYCLONES*. Weather Division. https://pubfiles.pagasa.dost.gov.ph/pagasaweb/files/tamss/weather/tcsummary/ARTC2018.pdf

Meneses III, S. F., & Blanco, A. C. (2022, May 31). RAPID MAPPING AND ASSESSMENT OF DAMAGES DUE TO TYPHOON RAI USING SENTINEL-1 SYNTHETIC APERTURE RADAR DATA. The International Archives of the Photogrammetry, Remote Sensing and Spatial Information Sciences, XLIII-B3-2022, 1139–1146. https://doi.org/10.5194/isprs-archives-xliii-b3-2022-1139-2022

What is remote sensing? (n.d.). NOAA's National Ocean Service. https://oceanservice.noaa.gov/facts/remotesensing.html

PAGASA. (2023). Dost.gov.ph. https://www.pagasa.dost.gov.ph/learning-tools/philippine-area-of-responsibility#:~:text=Philippine%20Area%20of%20Responsibility(PAR.closest%20to%20the%20Philippine%20Islands.

Profile of the region. (n.d.). CDA | Cooperative Development Authority. https://cda.gov.ph/region-1/about/

Sentinel-1 - Missions - Sentinel online - Sentinel online. (n.d.). Sentinel Online. https://sentinels.copernicus.eu/web/sentinel/missions/sentinel-1

MIMAROPA Region Profile – PhilAtlas. (1903, March 2). https://www.philatlas.com/luzon/mimaropa.html

NCR – About the Region | Department of Education. (n.d.). https://www.deped.gov.ph/regions/ncr/ncr-about-the-region/#:~:text=The%20National%20Capital%20Region%20(NCR,capital%20region%20of%20the%20Philippines.

Meneses, S. F. M., & Blanco, A. C. (2022, May 31). *RAPID MAPPING AND ASSESSMENT OF DAMAGES DUE TO TYPHOON RAI USING SENTINEL-1 SYNTHETIC APERTURE RADAR DATA*. The International Archives of the Photogrammetry, Remote Sensing and Spatial Information Sciences. https://doi.org/10.5194/isprs-archives-xliii-b3-2022-1139-2022

Zheng, Y., Shao, G., Tang, L., He, Y., Wang, X., Wang, Y., & Wang, H. (2019, July 19). *Rapid Assessment of a Typhoon Disaster Based on NPP-VIIRS DNB Daily Data: The Case of an Urban Agglomeration along Western Taiwan Straits, China*. Remote Sensing. https://doi.org/10.3390/rs11141709

Elvidge, C. D., Hsu, F. C., Zhizhin, M., Ghosh, T., & Sparks, T. (2023, January 5). *Statistical moments of VIIRS night-time lights*. International Journal of Remote Sensing. https://doi.org/10.1080/01431161.2022.2161857

Sentinel-1 polarization. (n.d.). Capella Space. https://support.capellaspace.com/hc/en-us/articles/360044738831-Sentinel-1-Polarization?fbclid=IwAR1yxQbQQlbO2JvFIctoV0Kv1GANo81MlV7yqHrjr18QSZhpq1ldkxaggVo

Nicolau, A. P., Flores-Anderson, A., Griffin, R., Herndon, K., & Meyer, F. J. (2021, February). Assessing SAR C-band data to effectively distinguish modified land uses in a heavily disturbed Amazon forest. *International Journal of Applied Earth Observation and Geoinformation*, *94*, 102214. https://doi.org/10.1016/j.jag.2020.102214

Satellite characteristics: Orbits and swaths. (2015, November 20). Language selection - Natural Resources Canada / Sélection de la langue - Ressources naturelles Canada. https://natural-resources.canada.ca/maps-tools-and-publications/satellite-imagery-and-air-photos/tutorial-fundamentals-remote-sensing/satellites-and-sensors/satellite-characteristics-orbits-and-swaths/9283?fbclid=IwAR1CY3NhUf-cOh76CDfDLClSvABs_cIQRPt2Th-zlFDw8iJ6e9ApBDZKgkA

Parameters for downloading Sentinel-1 images from open access hub. (2022, November 20). Endless Curiosity. https://yenyiwu.wordpress.com/2021/03/10/parameters1/?fbclid=IwAR11AnPrXefwgpmfcyLodnrDhpIHSb0zOeSuZRX3cqyFE1_9hUgBYMiq94w

Band Definition | GIS Dictionary. (n.d.). https://support.esri.com/en-us/gis-dictionary/band?fbclid=IwAR16HeoXBmur2IbTB1DnIp5nkYV86tGa0i7GwgfWH4qAbjYMAEmYhX-el9U#:~:text=%5Bremote%20sensing%5D%20A%20wavelength%20range,from%20approximately%20625%2D740%20nanometers

Li, S., Cao, X., Zhao, C., Jie, N., Liu, L., Chen, X., & Cui, X. (2023, August 8). Developing a Pixel-Scale Corrected Nighttime Light Dataset (PCNL, 1992–2021) Combining DMSP-OLS and NPP-VIIRS. *Remote Sensing*, *15*(16), 3925. https://doi.org/10.3390/rs15163925

Sentinel-1 Algorithms. (n.d.). Google for Developers. https://developers.google.com/earth-engine/guides/sentinel1?fbclid=IwAR16KArauSthN6dEer7IzCl0RmeW5AMT2OKbsPBN1e6rTXLL7C3NQFG4Arc

Panic, M., Drobnjakovic, M., Stanojevic, G., Kokotovic-Kanazir, V., & Doljak, D. (2022). Nighttime lights-innovative approach for identification of temporal and spatial changes in population distribution. *Journal of the Geographical Institute Jovan Cvijic, SASA*, *72*(1), 51–66. https://doi.org/10.2298/ijgi2201051p

Shi, K., Yu, B., Huang, Y., Hu, Y., Yin, B., Chen, Z., Chen, L., & Wu, J. (2014, February 20). Evaluating the Ability of NPP-VIIRS Nighttime Light Data to Estimate the Gross Domestic Product and the Electric Power Consumption of China at Multiple Scales: A Comparison with DMSP-OLS Data. *Remote Sensing*, *6*(2), 1705–1724. https://doi.org/10.3390/rs6021705

VIIRS/NPP Daily Gridded Day Night Band 500m Linear Lat Lon Grid Night - LAADS DAAC. (n.d.). https://ladsweb.modaps.eosdis.nasa.gov/missions-and-measurements/products/VNP46A1/?fbclid=IwAR2y7dFix-WbH2HwwR5jUbECAVHA4bZT8bt78EguWCgkzvNiXgsUJFJ_iwM

Center, C. D. R. (2020, February 19). *Typhoon Ompong: Impact on Ilocos Region - Citizens Disaster Response Center | CDRC*. Citizens Disaster Response Center | CDRC. https://www.cdrc-phil.com/typhoon-ompong-impact-on-ilocos-region/?fbclid=IwAR1GMCneeM_nVxckN6TkNCamf6Ip_6osxvfnHRGh9S0PyEwDq3kRrIkXprc

Arceo, A. (2018, September 14). *Typhoon Ompong makes landfall in Cagayan*. RAPPLER. https://www.rappler.com/nation/weather/212032-typhoon-ompong-pagasa-forecast-september-15-2018-2am/?fbclid=IwAR1_qM3ptxoU1cTNIx9uawKdXCPt1SceI1VwIdCsy9xBJ7CFer7BCBkK-nw

Launio, C. C. (2020, December 28). *Effects of extreme weather events and coping mechanisms of smallholder highland farmers: The case of. . .* ResearchGate. https://www.researchgate.net/publication/350449276_Effects_of_extreme_weather_events_and_coping_mechanisms_of_smallholder_highland_farmers_The_case_of_Typhoon_Ompong_in_Benguet_Philippines?fbclid=IwAR14zjZga9Dow_Ze_VV0I--CEgXdYMcF-bb8Ir_k3lpgOQ-cX5_x-4Ym_Y4

Asian Disaster Reduction Center (ADRC). (n.d.). https://www.adrc.asia/view_disaster_en.php?NationCode&Lang=en&Key=2299&fbclid=IwAR1pSlYRm5AyS-KpAZiBjBa-Hycb0zw4un1DqpTcX8uvUrvykFw-XCcDeqQ

Hall, C. (2022, February 1). *Nighttime Lights*. Earthdata. https://www.earthdata.nasa.gov/learn/backgrounders/nighttime-lights?fbclid=IwAR3k5jnD2vNaW6yBkWUNQnEeCIXgVpe8-iT_7gRMLaFg7IktxpE14rNvUH4

Michez, A., Bauwens, S., Bonnet, S., & Lejeune, P. (2016c). Characterization of Forests with LiDAR Technology. In *Elsevier eBooks* (pp. 331–362). https://doi.org/10.1016/b978-1-78548-103-1.50008-x

Hall, C. (2022, February 1). *Nighttime lights*. Earthdata. https://www.earthdata.nasa.gov/learn/backgrounders/nighttime-lights

Our mission and vision. (n.d.). National Oceanic and Atmospheric Administration. https://www.noaa.gov/our-mission-and-vision

Calabarzon. (n.d.-c). DBpedia. https://dbpedia.org/page/Calabarzon#:~:text=Calabarzon%20(%2Fk%C9%91%CB%90l%C9%91%CB%90b%C9%91%CB%90r%CB%88z%C9%92n%2F)%2C%20formally,one%20highly%20urbanized%20city%2C%20Lucena.

Joselito Guianan Chan, Managing Partner, Chan Robles and Associates Law Firm. (n.d.-b). *CORDILLERA ADMINISTRATIVE REGION (CAR), REPUBLIC OF THE PHILIPPINES - CHAN ROBLES VIRTUAL LAW LIBRARY*. https://chanrobles.com/legal3car.html

Sharma, S. (2019b). Synthetic Aperture Radar (SAR) ImagesProcessing: A review. *ResearchGate*. https://www.researchgate.net/publication/334647017_Synthetic_Aperture_Radar_SAR_ImagesProcessing_A_Review?fbclid=IwAR3ZcujzIf0wVqMfXe9KiKMkR9yb7U682te9_p2Y9HHESz8PqCCyt4NGfYw

Hall, C. (2023, November 21). *What is Synthetic Aperture Radar?* Earthdata. https://www.earthdata.nasa.gov/learn/backgrounders/what-is-sar?fbclid=IwAR356kgqNd9YwP04xi9JT8QpD5buZ1i_qgrSlsChwLacsZHmb3TNkCr_WIs

Xiong, Q., Li, G., Yao, X., & Zhang, X. (2023). SAR-to-Optical image translation and cloud removal based on conditional generative adversarial networks: literature survey, taxonomy, evaluation indicators, limits and future directions. *Remote Sensing*, *15*(4), 1137. https://doi.org/10.3390/rs15041137

Strobl, E. (2020, January 22). *The Impact of Typhoons on Economic Activity in the Philippines: Evidence from Nightlight Intensity*. Asian Development Bank. https://www.adb.org/publications/impact-typhoons-philippines

Oxfam, local partners ready to respond as "highly threatening" Typhoon Mangkhut nears Philippines. (2021, April 27). Oxfam Aotearoa. https://www.oxfam.org.nz/news-media/media-releases/oxfam-local-partners-ready-respond-highly-threatening-typhoon-mangkhut-nears-philippines/?fbclid=IwAR2m9VCRmVKERV0nc4TvOu0z9IulmnQYfw-Qny2Or_4bIxL2lWXjjmWiQ58

SALT LAKE CITY. (2018, September 14). Typhoon Mangkhut Strikes the Philippines. *The Church of Jesus Christ of Latter-day Saints*. https://newsroom.churchofjesuschrist.org/article/typhoon-mangkhut-strikes-the-philippines?fbclid=IwAR19xqoSFi1oHIeh5c12ZTPxZaeNaNNNCJ2lM4ecHl_KFiBKdrqUfnDtNo4

Rivera, J. (2022, November 14). *List: Top 10 Strongest Typhoon that hit the Philippines*. Announcement Philippines. https://announcement.ph/list-top-10-strongest-typhoon-that-hit-the-philippines/?fbclid=IwAR2Va3pisfguGpLMxPiRjKYSkGs6bgshjyTA2qm6o2uy8yxSjbDb5rzrfas

Nasa, E. S. D. S. (2023, December 6). *EarthData | EarthData*. Earthdata. https://www.earthdata.nasa.gov/

Adriano, L. (2022, October 17). Neneng leaves P177.6-M damage in Ilocos Norte. Philippine News Agency. https://www.pna.gov.ph/articles/1186355?fbclid=IwAR3yfTRM-owLbHZZu0-9wRPsczW4o4q2uW-NsQbNGkKwqVygf1PUM3Hs5SM

Zero casualties, P2.3 billion initial "Ompong" damages in Ilocos Norte. (n.d.). https://ilocosnorte.gov.ph/index.php/news/zero-casualties-p2-3-billion-initial-ompong-damages-in-ilocos-norte?fbclid=IwAR0z-E-xnsuTUjKojunfXKJQ_NoIJdb57Ae6380_Cqv7XoX7y9iQx52OZjA

Center, C. D. R. (2020, February 19). *Final Report: Typhoon Ompong (Mangkhut) in Central and Northern Luzon 2018 - Citizens Disaster Response Center | CDRC*. Citizens Disaster Response Center | CDRC. https://www.cdrc-phil.com/final-report-typhoon-ompong-mangkhut-in-central-and-northern-luzon-2018/?fbclid=IwAR1F0uK2rLy87KLTwSFO5IryWn4Dbcsb5nLGl__5mZxuT3sbhqeRZ2WSev0

Pérez-Sindín, X. S., Chen, T. H. K., & Prishchepov, A. V. (2021, November 1). *Are night-time lights a good proxy of economic activity in rural areas in middle and low-income countries? Examining the empirical evidence from Colombia*. Remote Sensing Applications: Society and Environment. https://doi.org/10.1016/j.rsase.2021.100647

Night Light Data: An Innovative Way to Track Development. (n.d.). Development Asia. https://development.asia/insight/night-light-data-innovative-way-track-development?fbclid=IwAR1tA51zOgp1tsT5m9C7Bmtu82LKlAVMpFU57ZFShYXtLW-jPxTZ_MPsW7s

Ghaffarian, S., Farhadabad, A. R., & Kerle, N. (2020, July 1). *Post-Disaster Recovery Monitoring with Google Earth Engine*. Applied Sciences. https://doi.org/10.3390/app10134574

Ecosystem, C. D. S. (2023, October 6). *Copernicus Data Space Ecosystem - Europe's eyes on Earth*. Copernicus Data Space

Ecosystem. https://dataspace.copernicus.eu/?fbclid=IwAR0-E7PQ1mh8Yz2NG46VKT01exV2r3zfH04m7aGqIIE0AjbzUuRD12P1qgQ

Zheng, Y., Shao, G., Tang, L., He, Y., Wang, X., Wang, Y., & Wang, H. (2019, July 19). *Rapid Assessment of a Typhoon Disaster Based on NPP-VIIRS DNB Daily Data: The Case of an Urban Agglomeration along Western Taiwan Straits, China*. Remote Sensing. https://doi.org/10.3390/rs11141709

Alahmadi, M., Mansour, S., Dasgupta, N., & Martin, D. (2023). Using nighttime lights data to assess the resumption of religious and socioeconomic activities Post-COVID-19. *Remote Sensing*, *15*(4), 1064. https://doi.org/10.3390/rs15041064

Wang, N., Hu, Y., Li, X., Kang, C., & Lin, Y. (2023). AOD Derivation from SDGSAT-1/GLI Dataset in Mega-City Area. *Remote Sensing*, *15*(5), 1343. https://doi.org/10.3390/rs15051343

Night-Time light imagery reveals China's city activity during the COVID-19 pandemic period in early 2020. (2021). IEEE Journals & Magazine | IEEE Xplore. https://ieeexplore.ieee.org/abstract/document/9426448?fbclid=IwAR296yWkFVwWSS6SJBd1tXPwLsftWOfI5tT0c9lL78cAL7sZmB4NHLD0uzM

Wang, Z., Román, M. O., Kalb, V., Miller, S. D., Zhang, J., & Shrestha, R. (2021). Quantifying uncertainties in nighttime light retrievals from Suomi-NPP and NOAA-20 VIIRS Day/Night Band data. *Remote Sensing of Environment*, *263*, 112557. https://doi.org/10.1016/j.rse.2021.112557

Preliminary Studies on Recovering Communities from Typhoon using Radiance Measurement from VIIRS. (2021, November 23). IEEE Conference Publication | IEEE Xplore. https://ieeexplore.ieee.org/abstract/document/9768701/authors?fbclid=IwAR2WOuvh9-vmaJngN0-CXQ8tK827tNHcKDaZdjo-nGl3FzIklZScEc7b-y8#authors

Elvidge, C. D., Zhizhin, M., Hsu, F., & Baugh, K. (2013). What is so great about nighttime VIIRS data for the detection and characterization of combustion sources? *Proceedings of the Asia-Pacific Advanced Network*, *35*(0), 33. https://doi.org/10.7125/apan.35.5

Kogut, P. (2023b, November 20). *Geospatial Data Analytics & Satellite Imagery by EOSDA*. EOS Data Analytics. https://eos.com/#:~:text=EOS%20Data%20Analytics%20is%20one,%2C%20commercial%2C%20and%20scientific%20organizations.

GPS. (n.d.-b). https://education.nationalgeographic.org/resource/gps/

Oxford Languages and Google - English | Oxford Languages. (2022, August 12). https://languages.oup.com/google-dictionary-en/

What is Infrastructure | IGI Global. (n.d.). https://www.igi-global.com/dictionary/infrastructure-and-tourism-development/14632#:~:text=Chapter%203-,The%20basic%20physical%20and%20organizational%20structures%20and%20facilities%20(e.g.%20buildings,energy)%20and%20water%20and%20sanitation.

What is lidar? (n.d.). https://oceanservice.noaa.gov/facts/lidar.html#:~:text=Lidar%2C%20which%20stands%20for%20Light,variable%20distances)%20to%20the%20Earth.

Hall, C. (2023b, November 21). *What is Synthetic Aperture Radar?* Earthdata. https://www.earthdata.nasa.gov/learn/backgrounders/what-is-sar#:~:text=SAR%20is%20a%20type%20of,after%20interacting%20with%20the%20Earth.

Tropical cyclones. (2021, April 12). World Meteorological Organization. https://public-old.wmo.int/en/our-mandate/focus-areas/natural-hazards-and-disaster-risk-reduction/tropical-cyclones

PAGASA. (2022). *About Tropical Cyclones*. Www.pagasa.dost.gov.ph. https://www.pagasa.dost.gov.ph/information/about-tropical-cyclone

Nasa, E. S. D. S. (2023a, December 5). *VIIRS | EarthData*. Earthdata. https://www.earthdata.nasa.gov/sensors/viirs

Román, M. O., Wang, Z., Sun, Q., Kalb, V., Miller, S. D., Molthan, A., Schultz, L. A., Bell, J. R., Stokes, E. C., Pandey, B., Seto, K. C., Hall, D. K., Oda, T., Wolfe, R. E., Lin, G., Golpayegani, N., Devadiga, S., Davidson, C., Sarkar, S., . . . Masuoka, E. (2018). NASA's Black Marble nighttime lights product suite. *Remote Sensing of Environment*, *210*, 113–143. https://doi.org/10.1016/j.rse.2018.03.017